Comparison of supercritical fluid chromatographic methods to predict the skin permeability of pharmaceutical and cosmetic compounds

Grooten, Yasmine; Mangelings, Debby; Vander Heyden, Yvan

Published in:
Journal of Chromatography. A

DOI:
10.1016/j.chroma.2023.463855

Publication date:
2023

Comparison of supercritical fluid chromatographic methods to predict the skin permeability of pharmaceutical and cosmetic compounds

Yasmine Grooten, Debby Mangelings, Yvan Vander Heyden*

Vrije Universiteit Brussel (VUB), Department of Analytical Chemistry, Applied Chemometrics and Molecular Modelling, Laarbeeklaan 103, B-1090 Brussels, Belgium

*: Corresponding author

E-mail addresses: yasmine.grooten@vub.be (Y. Grooten), debby.mangelings@vub.be (D. Mangelings), yvan.vander.heyden@vub.be (Y. Vander Heyden)

Abstract

Supercritical fluid chromatography (SFC) was explored as an alternative for liquid chromatography to predict the skin permeability of pharmaceutical and cosmetic compounds. Nine dissimilar stationary phases were applied to screen a test set of 58 compounds. The experimental retention factors (log *k*), in addition to two sets of theoretical molecular descriptors, were applied to model the skin permeability coefficient. Different modelling approaches, i.e. multiple linear regression (MLR) and partial least squares (PLS) regression, were used. In general, the MLR models performed better than the PLS models for a given descriptor set. The results obtained on a cyanopropyl (CN) column provided the best correlation with the skin permeability data. The retention factors obtained on this column were included in a simple MLR model, together with the octanol-water partition coefficient and the number of atoms (r^2 = 0.81, RMSEC = 0.537 or 20.5% and RMSECV = 0.580 or 22.1%). The overall best MLR model included the chromatographic descriptor from a phenyl column and 18 descriptors (r^2 = 0.98, RMSEC = 0.167 or 6.2% and RMSECV = 0.238 or 8.9%). This model showed a good fit, on top of very good predictive features. However, stepwise MLR models with a reduced complexity could also be determined, with the best performance parameters obtained with the CN-column based retention and eight descriptors (r^2 = 0.95, RMSEC = 0.282 or 10.7% and RMSECV = 0.353 or 13.4%). SFC thus provides a suitable alternative to the liquid chromatographic techniques previously applied to model the skin permeability.

Keywords

Skin permeability, quantitative retention-activity relationship models, quantitative structure-activity relationship models, supercritical fluid chromatography

1. Introduction

The skin plays an important role in many functions of the human body, such as preserving homeostasis and forming a barrier between the external and internal environment, but also as a sensory organ. It consists of three main layers, i.e. the epidermis, dermis and subcutaneous layer, along with the appearance of several skin appendages (sweat glands, sebaceous glands and hair follicles) [1]. The stratum corneum, the outermost layer of the epidermis, is the most important permeation barrier of the skin. Its structure is often referred to as a 'bricks and mortar' model, built with keratin-packed corneocytes surrounded by a matrix of lipid bilayers [2]. These hydrophobic lipids are mostly composed of ceramides, cholesterol and long-chain free fatty acids. When the skin is exposed to chemical, pharmaceutical or cosmetic compounds, passive diffusion through the skin (and possibly into the systemic circulation) can occur. The skin permeability coefficient K_p (expressed in cm/s or cm/h) indicates the rate at which a compound passes the skin [3]. This value can be estimated through *in-vivo* and *in-vitro* tests, of which, for some, guidelines with standardized procedures have been provided [4]. However, drawbacks, such as ethical aspects, high variability and difficulties to extrapolate from animal to human skin, on top of the European ban on animal testing of cosmetics, have raised the need for alternative methods [4,5].

In-silico approaches may provide an alternative, applying quantitative structure-activity relationship (QSAR) models, in which a biological activity (in this case, the skin permeability) is modelled as a function of physicochemical and/or structural properties of compounds (expressed by theoretical descriptors) [6–8]. Furthermore, these theoretical descriptors can be combined with one or more experimental chromatographic descriptors. Retention on several reversed-phase liquid chromatographic (RPLC) systems has been applied in this context to model the skin permeability of compounds. Besides regular octadecyl columns [9], biomimicking systems have been applied to resemble the skin structure. Immobilized artificial membrane (IAM) columns, which contain phospholipid analogues (mostly phosphatidylcholine) covalently bound to the silica surface, have been used to model log K_p [10–14]. Furthermore, other stationary phases containing skin components, such as cholesterol [15,16], keratin [17] and collagen [18], have been applied for the same purpose.

Micellar liquid chromatography (MLC) is another important technique in modelling the skin permeability. Micelles are formed when a surfactant, in the mobile phase, is above its critical micelle concentration, resulting in a pseudo-phase with which solutes can interact [19]. The chromatographic descriptors, obtained with either the anionic surfactant sodium dodecyl sulfate (SDS) or the nonionic Brij-35 (for the latter the term biopartitioning micellar chromatography (BMC) has been defined), have been used in skin permeability models [20–23]. Furthermore, thin-layer chromatography has been explored recently to model skin permeability [24–26].

Supercritical fluid chromatography (SFC) increased in popularity over the last years because of its many advantages. The mobile phase consists of a supercritical or subcritical fluid, which shows a low viscosity and high diffusivity, allowing the application of higher flow rates and thus fast analyses [27]. Most frequently, the non-toxic, non-polar and inert carbon dioxide (CO_2), which reaches its supercritical state at a rather low temperature and pressure (31°C and 74 bar, respectively), is the main compound in the mobile phase [28]. The polarity of CO_2 can be increased by the addition of more polar modifiers, e.g. methanol, ethanol and acetonitrile. Because lower modifier fractions are needed than in liquid chromatography (LC), lower solvent consumption is achieved [29]. As the stationary phase, all types used in liquid chromatography (ranging from polar to non-polar) can be applied in SFC. Furthermore, some, e.g. with a 2-ethylpyridine (2-EP) modification, were developed specifically for SFC [30,31]. Column selection for method development is therefore often challenging. Classification systems, indicating similarities and dissimilarities between stationary phases, may provide a solution. West et al. [32] applied linear solvation energy relationship (LSER) models in this context, characterizing column types in SFC by certain physicochemical properties. Galea et al. [33] proposed a set of six dissimilar stationary phases (selected out of 27), suitable for method development for pharmaceutical compounds in SFC. Selection was based on the application of the Kennard and Stone algorithm on the retention-factor matrix from test set compounds and on the resulting principal component analysis (PCA) plots.

In previous studies, we built skin-permeability predicting models using two sets of molecular descriptors, and compared them to models containing both theoretical and chromatographic

descriptors obtained from various LC methods. The retention factors measured with an octadecyl column showed to contribute little to improve the models containing only theoretical descriptors [34]. Afterwards, an MLC method was applied on the same column type, both on a particle-based and on a monolithic column. Improvement of the models was noticed compared to the *in-silico* ones, with a preference for the monolithic-column retention because of its speed [35]. Three additional methods were further compared, i.e. on an IAM, a cholesterol-bonded (in HPLC), and a sub-2 µm C18 column (in UHPLC). Although the best correlation between the retention factors and the skin permeability coefficients was obtained for those from the IAM column, combining the UHPLC results with theoretical descriptors provided a better model, on top of being a faster analysis [36].

The aim of this study was to evaluate a new approach to model skin permeability, i.e. by using chromatographic descriptors obtained with SFC. To the best of our knowledge, this technique was not yet applied in this context. Given the fast and 'green' properties of SFC, it may provide an improved alternative to the descriptors previously obtained in HPLC and UHPLC. Several stationary phases were tested in SFC, to assess their applicability in the context of skin permeability modelling. The selection of the stationary phases was based on a set of dissimilar columns proposed by Galea et al. [33,37], plus a cholesterol-bonded column (because of its link to the skin structure). The test set from the previous studies, with 58 diverse pharmaceutical and cosmetic compounds, was analyzed. From using a generic gradient on a limited number of compounds, the isocratic methanol fraction in the mobile phase was determined on each column as the average fraction needed to elute the compounds of a subset. This mobile phase was then applied isocratically to screen the entire test set. The retention factors, and one of two sets of theoretical descriptors, from Vega ZZ and E-Dragon software, respectively, were thereafter used to model the skin permeability coefficient, log K_p. Both multiple linear regression (MLR) and partial least squares (PLS) regression were applied, after which the best models, containing the retention on one of the different stationary phases, were compared. Furthermore, the best skin permeability models were compared to the models obtained from the previous studies [34–36].

2. Materials and methods

2.1. *Chemicals and reagents*

CO_2 quality 4.5 (purity ≥ 99.995%) was purchased from Messer (Sint-Pieters-Leeuw, Belgium). HPLC grade methanol (MeOH) was from VWR Chemicals (Fontenay-sous-Bois, France). The test set was composed of 58 compounds with different physicochemical and pharmaceutical properties, comprising a relevant log *P* range (-1.13 to 4.45), equivalent to a pH dependent hydrophobicity log *D* range from -1.86 to 4.31 (calculated with Chemicalize (Chemaxon, Budapest, Hungary) at the pH of the skin, i.e. pH 5.5), and log K_p ranges from -5.52 to -0.24, taken from the literature [38–42] (see **Table 1** for an overview). While log *P* takes into account the distribution of neutral species of a compound in octanol and water, log *D* determines the ratio of both the neutral and ionized forms (= microspecies) of the compound in octanol and water (taking the pK_a and specified pH into consideration) as follows: D = [sum of concentration of microspecies]$_{octanol}$/[sum of concentration of all microspecies]$_{water}$. The test set compounds were obtained from Bios Coutelier (Brussels, Belgium), Certa (Braine-l'Alleud, Belgium), Diosynth (Oss, The Netherlands), Fluka (Neu-Ulm, Switzerland), Merck (Darmstadt, Germany) and Sigma-Aldrich (Steinheim, Germany), with a purity of at least 95%. Individual sample solutions of 0.1 mg/mL were prepared in MeOH. When no result was measured, higher concentrations (0.25, 0.5, 0.75 and 1.0 mg/mL) were analyzed.

2.2. *Instrumentation*

The analyses were performed on an ACQUITY Ultra Performance Convergence Chromatography (UPC²) instrument from Waters (Milford, MA, USA). The system consisted of a binary solvent delivery pump, a convergence manager, an external ACQUITY column oven without active pre-heating, an autosampler (with a fixed loop of 10 µL) and a photodiode array (PDA) detector. The sample compartment was kept at 10°C throughout the analyses. Empower 3 software (version 7.10, Waters) was used for data collection and processing. The nine stationary phases tested are shown in **Table 2**. They were obtained from Phenomenex (Torrance, CA, USA), Nacalai Tesque (Kyoto, Japan) and Waters.

2.3. Gradient screening for isocratic mobile-phase composition determination

A generic gradient was applied on a selection of compounds (covering the log *P* range of the test set) to determine the best MeOH fraction in the mobile phase for the isocratic screening of the entire test set. The gradient starts with a mixture of CO_2 with 5% MeOH, which is increased to 40% in 10 min. The latter fraction was held for 5 min, after which it was decreased again to 5% MeOH in 0.5 min. To recondition the column, 5% MeOH was kept for 2 min, which results in a total run time of 17.5 min. When the maximal allowable column pressure restricted the operating conditions, the upper gradient limit was decreased (e.g. to 20% MeOH). The modifier fraction C_e at which each compound elutes within the gradient can be calculated as:

$$C_e = C_i + \frac{C_f - C_i}{t_G}(t_R - t_d - t_0) \qquad \text{(Eq. 1)}$$

in which C_i and C_f correspond to the initial and final modifier fractions in the gradient, respectively, t_G is the gradient time, t_R the retention time of the analyzed compound, t_d the instrument dwell time and t_0 the column void time [43]. The average C_e value for all compounds was used to decide on the MeOH fraction in the isocratic mobile phase.

2.4. Experimental conditions

The test set was analyzed isocratically, applying a mobile phase consisting of CO_2 and MeOH, of which the fraction was determined from the gradient screening. A flow rate of 3.0 mL/min was applied, except for the ACQUITY UPC² BEH column (sub-2 µm particles) for which the flow rate was 1.5 mL/min. A backpressure of 150 bar and a temperature of 25°C were maintained. UV detection was carried out at 220 nm. The injection volume was 10 µL for most columns, except for the ACQUITY UPC² BEH column, where it was 2 µL. The compounds were injected in triplicate. Retention factors (k) were determined as $(t_R - t_0)/t_0$, with the first disturbance of the baseline as t_0.

2.5. *Data sources, software and data processing*

The skin permeability coefficients, originating from *in-vitro* tests, were obtained from a validated database [38], and were extended with those of some additional relevant compounds [39–42]. It should be noticed that combining permeability data from several references is not recommended. However, because of their limited availability, it is often not possible to acquire large test sets from one source. The Vega ZZ software (version 3.2.1.33) [44] provided a first set of molecular descriptors,

representing 21 physicochemical, geometrical and topological properties, such as the Virtual log *P*, number of atoms (*Atoms*), molecular weight and gyration radius. Additionally, the melting point from PubChem was included in this descriptor set [45]. A second set of 1666 descriptors was acquired using E-Dragon software [46]. The (nearly) constant descriptors were removed from this set, as well as the highly correlated ($r > 0.95$, retaining the descriptor with the highest correlation to log K_p), which reduced the number of descriptors to 408.

MLR modelling with the Vega ZZ descriptors was performed using the 'automatic linear regression' module in the Vega ZZ software. Descriptors, except the chromatographic, which presented an $r^2 < 0.10$ with log K_p were excluded from the modelling. Furthermore, collinear descriptors showing a variance inflation factor (VIF, calculated as $1/(1-r^2)$) above 5 were never combined in the MLR models. The best models with one to seven descriptors, which included the chromatographic descriptor, were compared.

Stepwise MLR and PLS modelling were carried out using m-files in MATLAB R2019b (The Mathworks, Natick, MA, USA). With the stepwise MLR approach, models were built, alternating a forward selection with a backwards deletion of descriptors, until the fit of the model was not further enhanced by the addition or exclusion of descriptors. The descriptors in these models are shown in the order they were selected during the stepwise approach. The best PLS model contained a number of latent variables, which was selected based on the lowest root mean squared error of leave-one-out cross validation.

All models were evaluated by their RMSECV and RMSEC (root mean squared error of cross validation and calibration, respectively), which quantified their predictive abilities and fit, respectively. The lower these values, the better the model. For both parameters, relative values to the average log K_p are also shown, allowing an easier comparison of models built with different numbers of compounds. Additionally, the determination coefficient r^2 between the predicted and experimental log K_p values was used to evaluate the predictive properties of the models. Hierarchical cluster analysis (HCA), applying m-files in MATLAB, was performed on the log *k* values, to visualize the (dis)similarities between the nine tested stationary phases. Scatter plots of the predicted versus the

194 experimental log K_p values were drawn with Graphpad Prism version 9.1.2 (GraphPad Software, San
195 Diego, CA, USA).

196 To reduce the complexity of the obtained stepwise MLR models with E-Dragon descriptors
197 different methods were implemented. First, the RMSECV versus model-complexity (i.e. number of
198 descriptors in the model) curves were looked at to evaluate whether the RMSECV values improved
199 considerably with the addition of each descriptor. This was assessed by calculating ΔRMSECV, as
200 $(RMSECV_{A-1} - RMSECV_A)/RMSECV_{A-1}$, with A the model complexity, for each subsequent pair.
201 When ΔRMSECV was larger than or equal to 0.02, the addition of an extra descriptor substantially
202 improved the model [47]. The RMSECV values can be estimated either by leave-one-out (LOO-CV),
203 or a k-fold CV. Additionally, simplified models may also be obtained by determining a maximal
204 value, $RMSECV_{Crit}$, which does not differ significantly from the minimal RMSECV, $RMSECV_{Min}$,
205 [48,49]:

206 $$RMSECV_{Crit}^2 = F_{(\alpha, N, N)}\, RMSECV_{Min}^2 \qquad \text{(Eq. 2)}$$

207 $F_{(\alpha, N, N)}$ is at significance level $\alpha = 0.05$ and with N, N degrees of freedom (N being the number of
208 compounds in the training set).

209 **3. Results and discussion**

210 *3.1. Chromatographic measurements*

211 The set of 58 pharmaceutical and cosmetic compounds was analyzed on nine stationary phases. In a
212 first step, the methanol fraction in the mobile phase (calculated with Eq. 1) was determined using a
213 generic gradient and a smaller test set. For the Cholester, cyanopropyl (CN) and pentafluorophenyl
214 (PFP) columns, a CO_2/MeOH, 95/5 v/v mobile phase was selected. For the other stationary phases a
215 higher fraction of MeOH was preferred: CO_2/MeOH, 90/10 v/v. These mobile phases were applied to
216 screen the entire test set in isocratic mode. An overview of the obtained retention factors on each
217 column can be consulted in **Table S1** of the Supplementary material.

218 Hierarchical cluster analysis (HCA) was performed to visualize the dissimilarities between the
219 stationary-phase types. The weighted pair group method using arithmetic averages (WPGMA)

clustering was applied to link the columns using their log *k* values. The dissimilarity between the stationary phases was expressed as 1-|*r*|, with *r* the correlation coefficient. Only the compounds that showed a result on all nine columns, i.e. 51 compounds, could be included in this analysis. The resulting dendrogram is shown in **Fig. 1**. Three main clusters can be observed. In a first, the silica and BEH columns show great similarity, as they are clustered very low in the dendrogram. Both stationary phases consist of bare silica, resulting in similar retention profiles. Furthermore, these two columns are clustered with the CN and diol columns, which contain polar groups on their silica surface. A second cluster is composed of two stationary phases with basic properties, containing a pyridine (2-EP) and amino (NH_2) group. These two columns are slightly higher clustered with the more non-polar Cholester column. In the third cluster, containing the PFP and phenyl columns, the similarity can again be attributed to the column chemistries: both columns contain aromatic groups on their silica base. This third cluster is linked relatively high to the first two, showing more dissimilarities in the retention properties. When comparing the dendrogram with previous stationary-phase classifications [32,50], a large resemblance is noticed for the two main clusters, i.e. a distinction can be made between the polar (the two sub-clusters on the left side of **Fig. 1**), and the non-polar and aromatic stationary phases (represented by the PFP and phenyl columns). These previous studies situated the Cholester column in the latter main cluster, unlike the present study. However, in the polar cluster, the Cholester column is the most dissimilar.

Next, the correlation between the retention factors (log *k*) and the skin permeability (log K_p) was assessed. The equations and corresponding statistical parameters for the linear regressions (log K_p = a log $k + b$) are shown in **Table 3**. An inversely proportional relationship between the log *k* and log K_p values can be noticed. This observation means that compounds with higher skin permeability values, show lower retention and thus less affinity for the more polar (or intermediately polar) stationary phases applied in this study. Furthermore, for the Cholester, 2-EP and NH_2 columns a low correlation with the skin permeability (low r^2 values) was observed. These observations confirm the dendrogram in **Fig. 1**, in which these three column types are part of the same cluster. Thus, there are similarities in their retention profiles, which however showed less correlation with the skin permeation of these

compounds. On the other hand, the CN column provided the best correlation with the log K_p values, followed by the BEH, phenyl and diol columns. Even though the silica and BEH columns showed high similarities in their retention profiles, a slightly better correlation with the skin permeability was noticed for the BEH column. While some stationary phases showed promising results, the calibration and prediction errors (RMSEC and RMSECV, respectively) are quite high. Therefore, theoretical descriptors were added to the models to improve the modelling of the skin permeability.

3.2. MLR modelling with Vega ZZ descriptors

First, Vega ZZ descriptors were applied to enhance the skin permeability models containing the log *k* values. Multiple linear regression models were set up containing from one to seven descriptors for every stationary phase. The best of these models can be consulted in **Tables S2 to S10** in the Supplementary material. When adding more descriptors to the model, a better fit was noticed (lower RMSEC), together with an improvement of its predictive qualities (decreasing RMSECV). However, at a certain complexity, overfitting of the model occurs, resulting in worse predictive properties (higher RMSECV). The best number of descriptors is thus selected as a compromise between a good fit (RMSEC) and the predictive capacities (RMSECV) of the model.

An overview of the best MLR models with the chromatographic descriptor from each stationary phase and Vega ZZ descriptors is presented in **Table 4**. It can be noticed that all models include the Virtual log *P* as a descriptor. Furthermore, the number of atoms (*Atoms*) is selected in seven out of the nine best models. In correspondence with the results from section 3.1., the models with the Cholester, 2-EP and NH_2 descriptors were of a slightly lower quality (Eqs. 3, 5 and 8 in **Table 4**, respectively). Furthermore, the best models for these columns were more complex (including five to six descriptors) than the models built with the other chromatographic descriptors. On the other hand, in accordance with the correlation between the retention factors log *k* and the log K_p values, the overall best model was obtained with the CN descriptor (Eq. 6 in **Table 4**), containing only two other descriptors, the Virtual log *P* and the number of atoms (*Atoms*), besides log k_{CN}. This simple model shows large similarity to the model of Potts and Guy [51], which used the molecular weight and log *P* to predict skin permeability coefficients. Considering the high correlation between the molecular weight and

number of atoms (r = 0.95 with the current test set), these models are similar. The predicted log K_p values of this model are shown as a function of the experimental in **Fig. 2A**. Another descriptor that also performed well was from the diol column, when combined with three Vega ZZ descriptors (Virtual log *P*, number of atoms and Broto's Lipole) (Eq. 9 in **Table 4**).

The MLR (Vega ZZ/CN) model (Eq. 6) was compared to the best models obtained in previous studies with the same test set. The actual model showed an improvement compared to the best MLR model containing only Vega ZZ descriptors, i.e. the MLR (Vega ZZ) model (four descriptors, RMSEC = 0.690 or 25.7%, RMSECV = 0.752 or 28.0% and r^2 = 0.69) [34], indicating the added value of the current chromatographic descriptor. Moreover, further improvement is noticed relative to the best models containing a chromatographic descriptor, from two previous studies, i.e. to the MLR (Vega ZZ/MLC on a monolithic column) model (four descriptors, RMSEC = 0.670 or 25.0%, RMSECV = 0.734 or 27.4% and r^2 = 0.72) [35] and to the MLR (Vega ZZ/IAM) model (four descriptors, RMSEC = 0.636 or 23.7%, RMSECV = 0.702 or 26.1%, r^2 = 0.74) [36].

3.3. Stepwise MLR modelling with E-Dragon descriptors

The E-Dragon descriptors were used as a second set of descriptors to model the skin permeability, together with the chromatographic descriptors from each tested stationary phase, using a stepwise MLR approach. An overview of the models that selected a log *k* is provided in **Table 5**. The stationary phases for which the chromatographic descriptor was not selected by the stepwise approach (silica, PFP and Cholester column) were not included in this table. The number of selected descriptors ranged from 9 to 19, showing higher complexity in comparison to the models built with the Vega ZZ descriptors. This can also be attributed to the size of the descriptor sets (408 E-Dragon vs 22 Vega ZZ descriptors).

The best model was obtained with the results from the phenyl column (Eq. 16), showing very good parameters for its fit and predictive properties. The plot of the predicted versus the experimental log K_p values for this model is shown in **Fig. 2B**. It can be observed that the regression line through the data points and the bisector almost coincide. Furthermore, all data points are situated close to the

regression line. However, with 19 descriptors, this model is also the most complex. The MLR (E-Dragon/CN) model provided a good alternative, with a total of 12 descriptors (Eq. 13). Models which performed less good were those composed with the results from the 2-EP and NH_2 columns (Eqs. 12 and 14, respectively). Both models include nine descriptors, which often are the same (seven out of the eight descriptors selected, besides log *k*, are identical). However, it should be noted that even the less good performing models with this stepwise approach still show better statistical parameters than the MLR models built with the Vega ZZ descriptors.

The current best stepwise MLR model, i.e. MLR (E-Dragon/Phenyl) performed also better than the MLR (E-Dragon) model (ten descriptors, RMSEC = 0.378 or 14.1%, RMSECV = 0.452 or 16.8% and r^2 = 0.91) from a previous study [34]. A similar enhancement of the performance parameters was noticed relative to the best MLR (E-Dragon/MLC) model (ten descriptors, RMSEC = 0.329 or 12.4%, RMSECV = 0.399 or 15.0% and r^2 = 0.93) [35]. On the other hand, similar results were obtained as for the best MLR (E-Dragon/UHPLC) model (16 descriptors, RMSEC = 0.177 or 6.6%, RMSECV = 0.245 or 9.2% and r^2 = 0.98) [36].

3.4. Reducing the complexity of the MLR models

The stepwise MLR models built with E-Dragon descriptors are rather extensive, containing from 9 to 19 descriptors, and risk to be overfitting. This should be avoided when using the models in 'real-life' circumstances, e.g. for the prediction of the skin permeability of potential drug candidates. It is essential that the models also predict well for new compounds. Therefore, it was examined whether the MLR models could be simplified, while maintaining their performance quality. A first approach consisted of evaluating the RMSECV vs model complexity by assessing whether $\Delta RMSECV \geq 0.02$ for each descriptor added to a simpler model. This may be done with both the results from LOO-CV or k-fold CV, where the latter may provide a better indication of a possible overfitting of the models [52]. A second approach is based on calculating an $RMSECV_{Crit}$ value (Eq. 2). Since the aim was to obtain simpler models, which still contain a chromatographic descriptor, the number of descriptors could be barely decreased for the models containing the retention on the 2-EP and NH_2-bonded phases. In both

cases, the chromatographic descriptor was selected as the eighth of nine. Therefore, these simplified models were not discussed.

The MLR (E-Dragon/CN) model (Eq. 13 in **Table 5**) contains 12 descriptors. When examining ΔRMSECV, both with LOO-CV and k-fold CV, the addition of every descriptor to the model was justified. However, considering the $RMSECV_{Crit}$ value from LOO-CV, the model could be reduced to nine descriptors:

$$\log K_p = -2.08 - 1.23 \log k_{CN} - 0.49\ nHAcc + 0.12\ Rww - 1.36\ L3m - 0.51\ ALOGPS\_logS - 0.13\ H\text{-}051 - 0.35\ IDDE + 0.43\ Mor07m + 0.96\ Mor17p \quad \text{(Eq. 18)}$$

with RMSEC = 0.282 (10.7%), RMSECV = 0.353 (13.4%) and r^2 = 0.95 (n = 53).

This simplified model still displays very good performance parameters compared to the initial model. Furthermore, it performs better than the equivalent MLR (Vega ZZ/CN) model (Eq. 6 in **Table 4**).

Next, the MLR (E-Dragon/Diol) model (ten descriptors, see Eq. 15 in **Table 5**) was evaluated. The ΔRMSECV values obtained with LOO-CV, indicated a simplification to two descriptors. Since this drastically and dramatically impacted the performance parameters, the results are not shown. In contrast, the same approach based on k-fold CV showed that the addition of the seventh descriptor did not sufficiently improve the RMSECV values, thus leading to a model with six descriptors:

$$\log K_p = -1.48 + 0.30\ C\text{-}025 - 0.95 \log k_{Diol} + 0.30\ ALOGPS\_logP - 0.97\ EEig01r + 0.89\ Jhetp + 52.19\ R8v+ \quad \text{(Eq. 19)}$$

with RMSEC = 0.390 (14.6%), RMSECV = 0.449 (16.8%) and r^2 = 0.90 (n = 56).

The same reduction in model complexity was made considering the $RMSECV_{Crit}$ value. The performance parameters of the simplified model were similar to those of the original, and still better than those of the corresponding MLR (Vega ZZ/Diol) model (Eq. 9 in **Table 4**).

The most complex, but best performing model was the MLR (E-Dragon/Phenyl) model (Eq. 16 in **Table 5**). However, with a total of 19 descriptors, the risk of overfitting is high. The experimental descriptor was selected as sixth, thus requiring the simplified model to contain at least this number of

descriptors. Considering ΔRMSECV with LOO-CV, the model could be reduced to 15 descriptors, while applying k-fold CV showed that the addition of a 10th descriptor did not further improve the RMSECV value. The model with nine descriptors is:

$$\log K_p = -3.39 - 0.25\ RDF020e + 0.44\ C\text{-}025 - 0.00048\ SRW09 - 0.013\ D/Dr06 + 11.39\ JGI4 - 1.39 \log k_{Phenyl} - 0.83\ ALOGPS\_logS + 0.22\ H\text{-}047 - 0.92\ nBnz \quad \text{(Eq. 20)}$$

with RMSEC = 0.382 (14.2%), RMSECV = 0.482 (18.0%) and $r^2 = 0.91$ ($n = 58$).

This distinct reduction in number of descriptors leads to a decreased quality of the performance parameters. However, they were still similar to those of the other simplified models. Furthermore, this simpler model performed better than the corresponding MLR (Vega ZZ/Phenyl) model (Eq. 10 in **Table 4**). When applying the $RMSECV_{Crit}$ value, only a reduction to 17 descriptors can be made. However, because of the limited decrease in complexity, this model was not explored further.

The MLR (E-Dragon/BEH) model contained nine descriptors (Eq. 17 in **Table 5**). The ΔRMSECV showed the added value of each subsequent descriptor in the model, both in case of LOO-CV and k-fold CV. However, the number of descriptors could be decreased considering the $RMSECV_{Crit}$ value (with LOO-CV), leading to a model with five descriptors:

$$\log K_p = -2.83 + 0.54\ ALOGP - 0.84 \log k_{BEH} - 0.25\ nCs - 2.19\ E2s + 1.17\ MATS2p \quad \text{(Eq. 21)}$$

with RMSEC = 0.415 (15.8%), RMSECV = 0.476 (18.1%) and $r^2 = 0.89$ ($n = 54$).

Once more, the slight decrease in the quality of the performance parameters still resulted in a better model than the corresponding MLR (Vega ZZ/BEH) model (Eq. 11 in **Table 4**).

It can be concluded that it is possible to obtain simpler versions of the MLR models to predict skin permeability with acceptable quality. The best simplified model was obtained with the results on the CN column (Eq. 18). **Fig. 2C** shows the predicted versus the experimental log K_p values for this model, in which a strong resemblance is seen between the bisector and the regression line through the data points. Although the MLR (E-Dragon/Phenyl) model initially was the best, it is now observed that the simplified MLR (E-Dragon/CN) version performed better than the simplified MLR (E-

Dragon/Phenyl) model. These latter two models can be directly compared because they both contain the same number of descriptors.

Each simplified model still was better than the corresponding model including Vega ZZ descriptors. However, it could be noticed that these Vega ZZ models still contained less descriptors than the simplified E-Dragon models. This observation could be attributed to the limited number of descriptors in the Vega ZZ set compared to the E-Dragon one (22 vs 408 descriptors, respectively), providing less potential to obtain models with satisfactory quality.

Compared to the best stepwise MLR models obtained in previous studies [34–36], the simplified MLR (E-Dragon/CN) model (Eq. 18) performed better than the MLR (E-Dragon) and MLR (E-Dragon/MLC) models (parameters shown in section 3.3.). However, its performance parameters did not surpass those of the MLR (E-Dragon/UHPLC) model (parameters shown in section 3.3), nor those of the MLR (E-Dragon/IAM) (14 descriptors, RMSEC = 0.225 or 8.4%, RMSECV = 0.298 or 11.1%, and r^2 = 0.97) and MLR (E-Dragon/Cholester in HPLC) (16 descriptors, RMSEC = 0.232 or 8.6%, RMSECV = 0.304 or 11.3% and r^2 = 0.97) models. Nevertheless, similar performance parameters were obtained to the simplified versions of the latter three models [36].

3.5. PLS modelling

As an alternative to the MLR modelling, PLS modelling was applied to both the Vega ZZ and the E-Dragon descriptor sets, combined with the experimental descriptor from the SFC analyses. The number of latent variables in the model was selected based on the lowest RMSECV value (with LOO-CV). The results for the best PLS models with each stationary phase are shown in **Table 6**. The best PLS model built with Vega ZZ descriptors contained also the results from the CN column. For this model, nine PLS factors were selected. The predicted log K_p values were plotted against the experimental in **Fig. 2D**. They show more scatter around the regression line for the lower skin permeability values. Furthermore, it should be remarked that when using other chromatographic descriptors, less latent variables were selected, ranging from five to seven PLS factors. The PLS (Vega ZZ/Cholester) and PLS (Vega ZZ/NH_2) models fitted least good, while the PLS

(Vega ZZ/BEH) model showed the least good predictive qualities (RSMECV value). Besides the PLS models obtained with the CN and diol descriptors (the most complex models), the other models presented a lower performance quality.

The best PLS and MLR (Eq. 6 in **Table 4**) models with Vega ZZ descriptors were both obtained with the descriptor from the CN column. The PLS model performs slightly less good, especially when looking at the RMSECV value. In comparison to the corresponding best PLS (Vega ZZ) model (five PLS factors, RMSEC = 0.757 or 28.2%, RMSECV = 0.807 or 30.0% and r^2 = 0.63) [34], the PLS (Vega ZZ/CN) model showed better performance parameters. The same observation is made when comparing this model to the best PLS (Vega ZZ/MLC) model (monolithic column, seven latent variables, RMSEC = 0.683 or 25.6%, RMSECV = 0.797 or 29.9%, r^2 = 0.70) [35] on the one hand, and the PLS (Vega ZZ/IAM) model (six latent variables, RMSEC = 0.674 or 25.1%, RMSECV = 0.763 or 28.4% and r^2 = 0.71) [36] on the other.

The same approach applied on the E-Dragon descriptors resulted in a number of PLS factors varying between six and nine (**Table 6**). Overall, for most stationary phases an improved model fit (lower RMSEC and higher r^2) is noticed compared to the PLS models with the Vega ZZ descriptors. However, the increased RMSECV values of the E-Dragon PLS models mean that their predictive capacities were less good. Again, the best PLS model is associated with the most latent variables, i.e. the PLS (E-Dragon/Silica) model (nine PLS factors), for which a clearly better fit is noticed than for the PLS (Vega ZZ/CN) model. The model risks to be overfitting given its complexity and much less good predictive properties (high RMSECV relative to RMSEC). In **Fig. 2E** it is again seen that the most challenging compounds to model are those with lower log K_p values. The RMSECV value of the PLS (Vega ZZ/CN) model was better than that of this model. Moreover, the best PLS model does not surpass the parameters of the MLR (E-Dragon/Phenyl) model (Eq. 16 in **Table 5**), nor the best simplified MLR (E-Dragon/CN) model (Eq. 18). A similarly performing PLS model with E-Dragon descriptors was obtained for the CN column, selecting eight PLS factors. On the other hand, the other PLS models showed a comparable less good fit, while the worst RMSECV values were obtained for the PFP and BEH columns (all selecting six PLS factors).

Compared to the best PLS (E-Dragon) model (six PLS factors, RMSEC = 0.674 or 25.1%, RMSECV = 0.860 or 32.0% and r^2 = 0.72) [34], the PLS (E-Dragon/Silica) model showed an improved result. However, the performance parameters did not surpass those of the PLS (E-Dragon/MLC) model (particle-based column with nine PLS factors, RMSEC = 0.421 or 15.8%, RMSECV = 0.730 or 27.4%, r^2 = 0.89) [35], nor of the PLS (E-Dragon/Cholester in HPLC) model (ten PLS factors, RMSEC = 0.424 or 15.7%, RMSECV = 0.854 or 31.7% and r^2 = 0.89) [36].

4. Conclusions

In this paper, SFC was introduced as a new alternative to the previously tested HPLC and UHPLC techniques to model skin permeability. In this context, nine stationary-phase types were screened in SFC using a test set of 58 pharmaceutical and cosmetic compounds. The best correlation between the retention factors (log k) and the skin permeability coefficient (log K_p) was obtained with the CN column. The retention on this column also provided one of the best models with each modeling approach. The log k_{CN} in combination with Vega ZZ descriptors Virtual log P and number of atoms provided the best MLR model. In this way, a simple model was obtained, which showed resemblance to the skin permeability model introduced by Potts and Guy [51]. The overall best model in this study was obtained with the stepwise MLR approach and contains 18 E-Dragon descriptors and log k_{Phenyl}. Both for the fit and the predictions, this model performed very well with relative errors below 10%. The complexity of most MLR models built with E-Dragon descriptors could be reduced without dramatically impacting the quality of their performance. Among the latter, the MLR (E-Dragon/CN) model, including nine descriptors, provided the best result. For a given descriptor set, the MLR models were better than the corresponding PLS models.

When comparing the best models with those from previous studies [34–36], it can be concluded that the current MLR models performed better. The PLS model built with the Vega ZZ descriptors also did. The best simplified MLR model was not better than the best MLR (E-Dragon/UHPLC), MLR (E-Dragon/IAM) and MLR (E-Dragon/Cholester in HPLC) models. However, its performance parameters were similar to the simplified versions of the latter three models. Furthermore, the best PLS (E-Dragon/Silica) model did not surpass the performance parameters of the previously obtained

456 best PLS models, except for the PLS (E-Dragon) model. The overall best model was the stepwise
457 MLR (E-Dragon/Phenyl) model.

458 It can be concluded that several stationary phases in SFC provide a suitable alternative for the
459 currently used RPLC methods to predict skin permeability. Furthermore, only 5 or 10% methanol was
460 needed as organic modifier in the mobile phase, attributing to the 'green' character of the proposed
461 methods. However, it should be noted that the currently obtained models should be further validated,
462 preferably with an extended external test set.

463 **Acknowledgments**

464 Y.G. is funded by a Ph.D. fellowship of the Research Foundation Flanders (FWO) [grant 11D3518N].
465 The authors thank R. Verellen for technical assistance.

466 **Conflict of Interest**

467 The authors declare that they have no conflict of interest.

468 **Figures**

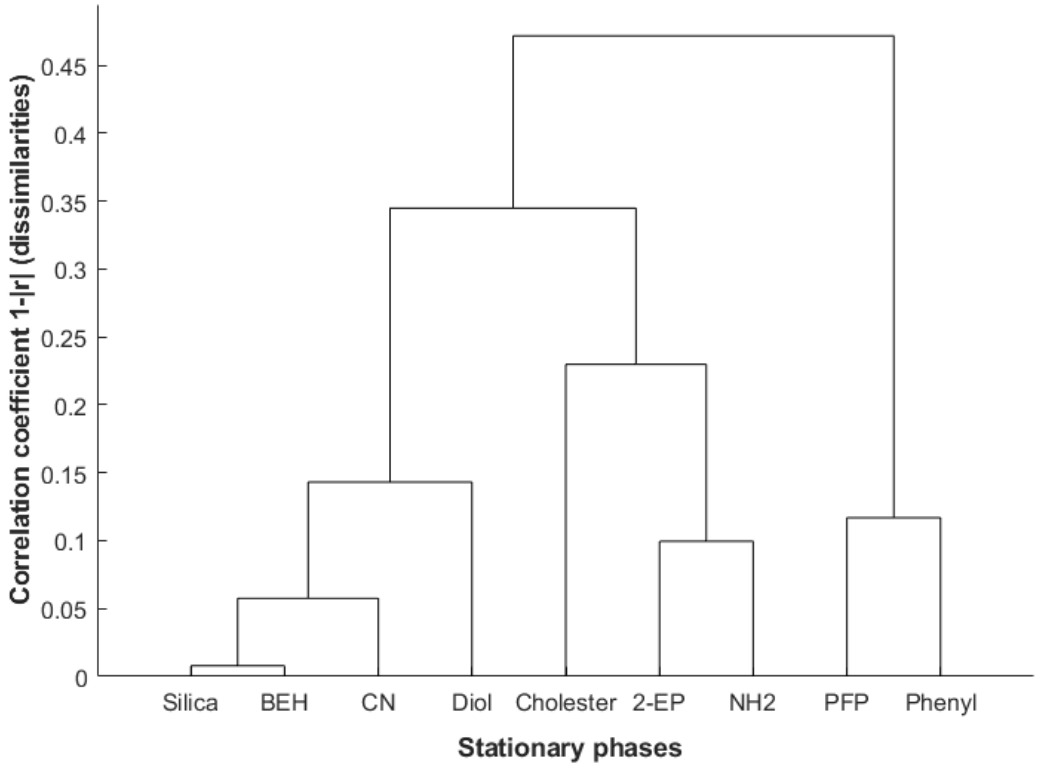

469

470 **Fig. 1.** Dendrogram based on WPGMA clustering, showing the (dis)similarities between the nine

471 tested stationary phases (using the log *k* values for 51 compounds).

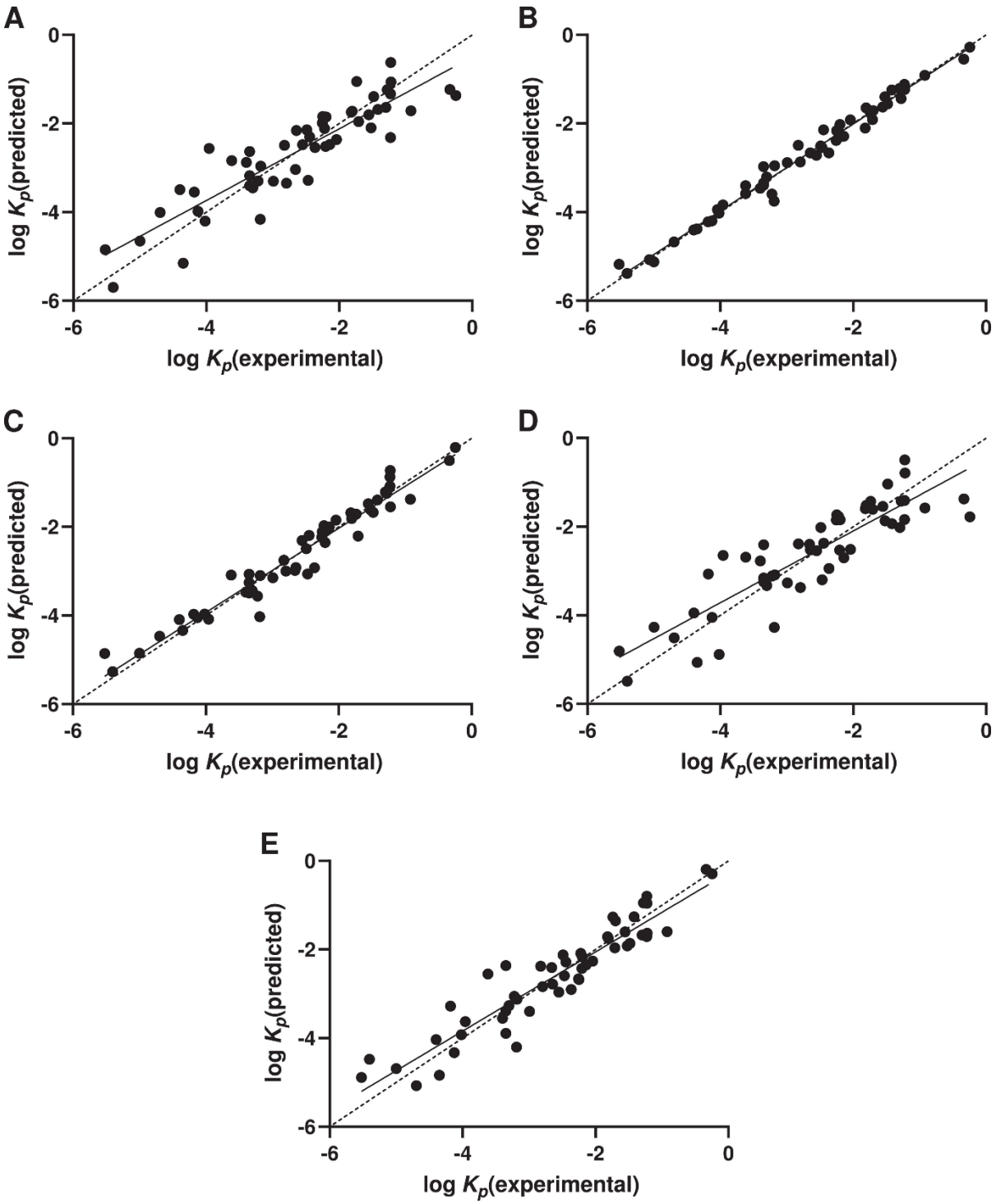

472

473 **Fig. 2.** The predicted versus the experimental log K_p values, together with the regression line (solid
474 line) and bisector (y = x, dashed line), for A) the MLR (Vega ZZ/CN) model (Eq. 6); B) the stepwise
475 MLR (E-Dragon/Phenyl) model (Eq. 16); C) the simplified stepwise MLR (E-Dragon/CN) model
476 (Eq. 18); D) the PLS (Vega ZZ/CN) model; and E) the PLS (E-Dragon/Silica) model.

Tables

Table 1. An overview of the compounds in the test set.

Compound	log *P* [a]	log *D* [b]	log K_p [c]	Company
17α-hydroxyprogesterone	1.84	3.40	-3.22	Sigma-Aldrich
2,4,6-Trichlorophenol	3.94	3.36	-1.23	Sigma-Aldrich
2,4-Dichlorophenol	3.18	2.87	-1.22	Sigma-Aldrich
2-Amino-4-nitrophenol	1.39	0.78	-3.18	Sigma-Aldrich
2-Nitro-p-phenylenediamine	0.78	0.90	-3.30	Sigma-Aldrich
4-Amino-2-nitrophenol	1.22	0.78	-2.55	Sigma-Aldrich
Acetylsalicylic acid	1.10	-0.84	-2.14 [39]	Sigma-Aldrich
Aminopyrine	1.57	1.14	-2.99	Sigma-Aldrich
Amylobarbital	1.97	1.89	-2.64	Bios
Antipyrine	1.26	1.22	-4.18	Unknown origin
Atropine	2.14	-1.78	-5.07	Sigma-Aldrich
Barbital	0.95	0.71	-3.96	Bios Coutelier
Benzoic acid	1.24	0.19	-1.52	Merck
Benzyl alcohol	1.34	1.21	-2.22	Sigma-Aldrich
Caffeine	-0.25	-0.55	-2.80	Fluka
Chloroxylenol	3.06	3.30	-1.23	Sigma-Aldrich
Chlorpheniramine (maleate)	3.86	0.21	-2.66	Sigma-Aldrich
Cortexolone	0.97	2.58	-4.12	Sigma-Aldrich
Cortexone	1.92	3.33	-3.35	Sigma-Aldrich
Corticosterone	0.82	2.02	-3.19	Sigma-Aldrich
Cortisone	-0.12	1.66	-5.00	Sigma-Aldrich
Diclofenac	4.45	2.75	-1.74	Sigma-Aldrich
Ephedrine.HCl	1.73	-1.86	-2.22	Sigma-Aldrich
Estriol	2.30	2.67	-4.40	Unknown origin
Estrone	3.18	4.31	-2.44	Diosynth
Ethyl nicotinate	1.35	1.11	-2.20	Sigma-Aldrich
Flurbiprofen	3.88	2.83	-0.34	Sigma-Aldrich
Haloperidol	3.75	1.16	-4.04 [40]	Unknown origin
Hydrocortisone	0.01	1.28	-5.52	Certa
Ibuprofen	3.20	3.11	-0.24	Sigma-Aldrich
Indomethacin	4.04	1.82	-1.30	Sigma-Aldrich
Ketoprofen	2.23	1.99	-1.23	Sigma-Aldrich
Lidocaine	3.01	0.61	-1.70 [41]	Sigma-Aldrich
m-Cresol	2.09	2.18	-1.82	Sigma-Aldrich
Methyl nicotinate	0.93	0.76	-2.49	Sigma-Aldrich
Methyl-4-hydroxybenzoate	1.36	1.67	-2.04	Fluka
m-Nitrophenol	2.21	1.61	-2.25	Sigma-Aldrich
Naproxen	3.23	1.66	-1.42	Sigma-Aldrich
o-Chlorophenol	2.40	2.27	-1.48	Sigma-Aldrich
o-Cresol	2.07	2.18	-1.80	Sigma-Aldrich
Paracetamol	1.07	0.91	-3.35	Sigma-Aldrich
p-Cresol	2.16	2.18	-0.92	Sigma-Aldrich

Phenobarbitone	1.49	1.40	-3.35	Unknown origin
Phenol	1.59	1.67	-1.71	Merck
Piroxicam	1.59	0.03	-2.47	Sigma-Aldrich
p-Nitrophenol	2.17	1.60	-2.25	Sigma-Aldrich
p-Phenylenediamine	0.23	-0.67	-3.62	Sigma-Aldrich
Prednisolone	-0.45	1.27	-4.35	Sigma-Aldrich
Progesterone	2.85	4.15	-2.82	Sigma-Aldrich
Resorcinol	1.18	1.37	-3.62	Merck
Salicylic acid	0.96	-0.67	-2.20	Sigma-Aldrich
Testosterone	2.48	3.37	-3.40	Sigma-Aldrich
Thiourea	-0.65	-0.47	-4.02 [42]	Merck
Thymol	3.23	3.43	-1.28	Sigma-Aldrich
Triamcinolone	-1.13	0.24	-5.40	Sigma-Aldrich
Triamcinolone acetonide	1.40	1.94	-4.69	Sigma-Aldrich
β-estradiol	3.37	3.75	-2.37	Unknown origin
β-naphthol	2.61	2.66	-1.55	Merck

[a] Virtual log *P*, calculated using Vega ZZ

[b] pH dependent hydrophobicity, log *D*, calculated using Chemicalize at pH 5.5

[c] Skin permeability coefficient log K_p, taken from [38], unless a different source was indicated

Table 2. The stationary phases selected for this study and their specifications.

Stationary phase	Denotation	Column dimensions	Manufacturer	Description
Cosmosil Cholester	Cholester	150 mm x 4.6 mm i.d., 5 µm	Nacalai Tesque	Cholesteryl groups bound to silica
Luna Silica	Silica	100 mm x 4.6 mm i.d., 3 µm	Phenomenex	Bare silica
Viridis Silica 2-EP	2-EP	100 mm x 4.6 mm i.d., 5 µm	Waters	2-ethylpyridine groups bound to silica
Luna CN	CN	100 mm x 4.6 mm i.d., 3 µm	Phenomenex	Cyanopropyl groups bound to silica
Luna PFP	PFP	100 mm x 4.6 mm i.d., 3 µm	Phenomenex	Pentafluorophenylpropyl groups bound to silica
Luna NH_2	NH_2	100 mm x 4.6 mm i.d., 3 µm	Phenomenex	Aminopropyl groups bound to silica
Luna HILIC	Diol	100 mm x 4.6 mm i.d., 3 µm	Phenomenex	Cross-linked diol groups covering silica
Synergi Polar RP	Phenyl	100 mm x 4.6 mm i.d., 4 µm	Phenomenex	Phenyl-oxypropyl groups bound to silica
Acquity UPC² BEH	BEH	100 mm x 3 mm i.d., 1.7 µm	Waters	Ethylene bridged hybrid (BEH) silica

Table 3. Results of the modelling of the skin permeability coefficient log K_p as a function of the retention factors log k from the different stationary phases (log $K_p = a \log k + b$).

Stationary phase	*n*	RMSEC	RMSECV	r^2	*a*	*b*
Cholester	58	1.211 (45.1%)	1.251 (46.6%)	0.05	-0.68	-2.57
Silica	54	1.029 (39.5%)	1.094 (41.9%)	0.29	-1.34	-2.27
2-EP	58	1.218 (45.3%)	1.254 (46.7%)	0.04	-0.61	-2.42
CN	53	0.851 (32.4%)	0.903 (34.4%)	0.52	-1.65	-2.08
PFP	54	1.016 (38.6%)	1.066 (40.5%)	0.33	-1.83	-3.10
NH_2	57	1.223 (45.4%)	1.262 (46.8%)	0.05	-0.47	-2.37
Diol	56	0.997 (37.2%)	1.037 (38.7%)	0.37	-1.39	-2.31
Phenyl	58	0.982 (36.6%)	1.025 (38.1%)	0.38	-1.98	-2.44
BEH	54	0.975 (37.0%)	1.025 (38.9%)	0.38	-1.73	-2.78

n is the number of compounds included in the modelling, RMSEC and RMSECV the root mean squared error of calibration and of cross validation (together with their relative values), respectively, r^2 the determination coefficient, *a* the slope and *b* the intercept of the equation.

Table 4. The best MLR models built with Vega ZZ descriptors and the chromatographic descriptors from each stationary phase.

Column	*n*	RMSEC	RMSECV	r^2	Equation
Cholester	58	0.665 (24.8%)	0.737 (27.4%)	0.71	$\log K_p = -3.27 - 0.78 \log k_{Chol} - 0.038\ Atoms + 0.60\ Virtual\ log\ P + 0.23\ Lipole\ (Broto) + 0.12\ HbAcc$ (Eq. 3)
Silica	54	0.585 (22.4%)	0.649 (24.9%)	0.77	$\log K_p = -2.42 + 0.55\ Virtual\ log\ P - 0.0034\ Melting\ point - 0.48 \log k_{Silica} - 0.021\ Atoms$ (Eq. 4)
2-EP	58	0.663 (24.7%)	0.731 (27.2%)	0.72	$\log K_p = -2.86 - 0.75 \log k_{2\text{-}EP} - 0.048\ Atoms + 0.53\ Virtual\ log\ P + 0.28\ Lipole\ (Broto) + 0.17\ HbAcc$ (Eq. 5)
CN	53	0.537 (20.5%)	0.580 (22.1%)	0.81	$\log K_p = -2.58 - 0.88 \log k_{CN} + 0.53\ Virtual\ log\ P - 0.024\ Atoms$ (Eq. 6)
PFP	54	0.615 (23.4%)	0.695 (26.4%)	0.75	$\log K_p = -2.62 + 0.51\ Virtual\ log\ P - 0.76 \log k_{PFP} - 0.027\ Atoms - 0.24\ HbDon$ (Eq. 7)
NH_2	57	0.674 (25.0%)	0.768 (28.5%)	0.71	$\log K_p = -1.44 + 0.24 \log k_{NH2} - 0.0043\ Melting\ point + 0.63\ Virtual\ log\ P + 0.011\ PSA - 0.36\ HbDon - 0.70\ Gyration\ radius$ (Eq. 8)
Diol	56	0.555 (20.7%)	0.607 (22.7%)	0.81	$\log K_p = -2.75 + 0.49\ Virtual\ log\ P - 0.93 \log k_{Diol} - 0.029\ Atoms + 0.15\ Lipole\ (Broto)$ (Eq. 9)
Phenyl	58	0.621 (23.1%)	0.672 (25.0%)	0.75	$\log K_p = -2.92 + 0.49\ Virtual\ log\ P - 1.76 \log k_{Phenyl} - 0.0088\ PSA$ (Eq. 10)
BEH	54	0.607 (23.0%)	0.662 (25.1%)	0.76	$\log K_p = -2.88 + 0.56\ Virtual\ log\ P - 0.89 \log k_{BEH} - 0.029\ Atoms$ (Eq. 11)

HbAcc = number of hydrogen bond acceptors, *HbDon* = number of hydrogen bond donors, *PSA* = polar surface area.

n is the number of compounds included in the modelling, RMSEC and RMSEV the root mean squared error of calibration and of cross validation (together with their relative values), respectively, and r^2 the determination coefficient.

Table 5. The best stepwise MLR models including E-Dragon and chromatographic descriptors from the various stationary phases.

Column	*n*	RMSEC	RMSECV	r^2	Equation
2-EP	58	0.389 (14.5%)	0.470 (17.5%)	0.90	$\log K_p$ = -6.33 – 0.32 *RDF020e* + 0.81 *C-025* + 0.24 *RDF055p* – 0.00098 *SRW09* – 1.17 *G1u* – 0.0072 *D/Dr06* + 5.87 *JGI4* – 0.39 $\log k_{2\text{-}EP}$ + 1.27 *BEHm1* (Eq. 12)
CN	53	0.223 (8.5%)	0.282 (10.7%)	0.97	$\log K_p$ = -1.52 – 1.14 $\log k_{CN}$ – 0.57 *nHAcc* + 0.12 *Rww* – 1.51 *L3m* – 0.53 *ALOGPS_logS* – 0.16 *H-051* – 0.39 *IDDE* + 0.55 *Mor07m* + 1.79 *Mor17p* – 0.71 *Mor15u* + 0.058 *RDF065m* – 0.56 *G1u* (Eq. 13)
NH_2	57	0.388 (14.4%)	0.457 (17.0%)	0.90	$\log K_p$ = -7.62 – 0.32 *RDF020e* + 0.80 *C-025* + 0.25 *RDF055p* – 0.0010 *SRW09* – 0.90 *G1u* – 0.0075 *D/Dr06* + 1.65 *BEHm1* – 0.34 $\log k_{NH2}$ – 0.48 *MATS4e* (Eq. 14)
Diol	56	0.307 (11.5%)	0.368 (13.7%)	0.94	$\log K_p$ = -1.22 + 0.46 *C-025* – 1.02 $\log k_{Diol}$ + 0.19 *ALOGPS_logP* – 0.82 *EEig01r* + 0.61 *Jhetp* + 63.29 *R8v+* + 0.055 *G(N..N)* + 9.55 *JGI4* – 1.38 *HATS2u* + 0.48 *Mor13m* (Eq. 15)
Phenyl	58	0.167 (6.2%)	0.238 (8.9%)	0.98	$\log K_p$ = -3.82 – 0.13 *RDF020e* + 0.74 *C-025* – 0.00059 *SRW09* – 0.022 *D/Dr06* + 15.48 *JGI4* – 1.79 $\log k_{Phenyl}$ – 0.80 *ALOGPS_logS* + 0.24 *H-047* – 1.07 *nBnz* + 0.78 *EEig13x* + 23.51 *JGI7* – 0.034 *G(O..O)* + 0.25 *nCconj* – 0.26 *Mor09e* + 0.076 *RDF090e* – 0.83 *Mor20e* + 1.07 *MATS1m* + 0.22 *S3K* + 0.41 *H1m* (Eq. 16)
BEH	54	0.313 (11.9%)	0.387 (14.7%)	0.94	$\log K_p$ = -3.62 + 0.63 *ALOGP* – 1.36 $\log k_{BEH}$ – 0.25 *nCs* – 1.12 *E2s* + 2.06 *MATS2p* – 1.17 *L3m* + 0.072 *RDF065m* + 0.28 *Hy* – 0.46 *Mor18u* (Eq. 17)

n is the number of compounds included in the modelling, RMSEC and RMSEV the root mean squared error of calibration and of cross validation (together with their relative values), respectively, and r^2 the determination coefficient.

Table 6. The performance parameters for the PLS models with the Vega ZZ and the E-Dragon descriptors.

		Vega ZZ descriptors				**E-Dragon descriptors**			
Column	***n***	**# PLS factors**	**RMSEC**	**RMSECV**	r^2	**# PLS factors**	**RMSEC**	**RMSECV**	r^2
Cholester	58	5	0.757 (28.2%)	0.805 (30.0%)	0.63	6	0.674 (25.1%)	0.860 (32.0%)	0.72
Silica	54	5	0.705 (27.0%)	0.711 (27.3%)	0.67	9	0.431 (16.5%)	0.769 (29.5%)	0.88
2-EP	58	6	0.710 (26.4%)	0.812 (30.2%)	0.68	6	0.674 (25.1%)	0.860 (32.0%)	0.72
CN	53	9	0.590 (22.5%)	0.674 (25.7%)	0.77	8	0.470 (17.9%)	0.808 (30.8%)	0.85
PFP	54	5	0.727 (27.6%)	0.761 (28.9%)	0.66	6	0.648 (24.6%)	0.941 (35.7%)	0.74
NH_2	57	5	0.760 (28.2%)	0.798 (29.6%)	0.64	6	0.679 (25.2%)	0.867 (32.2%)	0.72
Diol	56	7	0.643 (24.0%)	0.720 (26.9%)	0.74	6	0.674 (25.2%)	0.877 (32.8%)	0.73
Phenyl	58	5	0.754 (28.1%)	0.791 (29.4%)	0.64	6	0.674 (25.1%)	0.860 (32.0%)	0.72
BEH	54	5	0.724 (27.5%)	0.814 (30.9%)	0.66	6	0.648 (24.6%)	0.941 (35.7%)	0.74

n: number of compounds included in the modelling, RMSEC and RMSEV: the root mean squared errors of calibration and cross validation (together with their relative values), respectively, r^2: the determination coefficient.

References

[1] K.A. Walters, M.S. Roberts, The Structure and Function of Skin, in: K.A. Walters (Ed.), Dermatological and Transdermal Formulations, CRC Press, Florida, USA, 2002: pp. 1–39.

[2] G.P. Moss, D.R. Gullick, S.C. Wilkinson, Predictive Methods in Percutaneous Absorption, Springer Verlag, Heidelberg, Germany, 2015.

[3] J. Kielhorn, S. Melching-Kollmuß, I. Mangelsdorf, Environmental Health Criteria 235: Dermal Absorption, World Health Organization Press, Geneva, 2006. https://inchem.org/documents/ehc/ehc/ehc235.pdf.

[4] R. Neupane, S.H.S. Boddu, J. Renukuntla, R.J. Babu, A.K. Tiwari, Alternatives to biological skin in permeation studies: Current trends and possibilities, Pharmaceutics. 12 (2020) 152. https://doi.org/10.3390/pharmaceutics12020152.

[5] J. Buzek, B. Ask, Regulation (EC) No 1223/2009 of the European Parliament and of the Council of 30 November 2009 on cosmetic products, Off. J. Eur. Union L. 342 (2009) 59–209.

[6] G.P. Moss, J.C. Dearden, H. Patel, M.T.D. Cronin, Quantitative structure – permeability relationships (QSPRs) for percutaneous absorption, Toxicol. in Vitro. 16 (2002) 299–317. https://doi.org/10.1016/S0887-2333(02)00003-6.

[7] S. Geinoz, R.H. Guy, B. Testa, P.A. Carrupt, Quantitative structure-permeation relationships (QSPeRs) to predict skin permeation: A critical evaluation, Pharm. Res. 21 (2004) 83–92. https://doi.org/10.1023/B:PHAM.0000012155.27488.2b.

[8] I. Tsakovska, I. Pajeva, M. al Sharif, P. Alov, E. Fioravanzo, S. Kovarich, A.P. Worth, A.N. Richarz, C. Yang, A. Mostrag-Szlichtyng, M.T.D. Cronin, Quantitative structure-skin permeability relationships, Toxicology. 387 (2017) 27–42. https://doi.org/10.1016/j.tox.2017.06.008.

[9] S. Soriano-Meseguer, E. Fuguet, A. Port, M. Rosés, Estimation of skin permeation by liquid chromatography, ADMET DMPK. 6 (2018) 140–152. https://doi.org/10.5599/admet.512.

[10] A. Nasal, M. Sznitowska, A. Buciński, R. Kaliszan, Hydrophobicity parameter from high-performance liquid chromatography on an immobilized artificial membrane column and its relationship to bioactivity, J. Chromatogr. A. 692 (1995) 83–89. https://doi.org/10.1016/0021-9673(94)00689-7.

[11] F. Barbato, B. Cappello, A. Miro, M.I. la Rotonda, F. Quaglia, Chromatographic indexes on immobilized artificial membranes for the prediction of transdermal transport of drugs, Il Farmaco. 53 (1998) 655–661. https://doi.org/10.1016/S0014-827X(98)00082-2.

[12] E. Lázaro, C. Ràfols, M.H. Abraham, M. Rosés, Chromatographic estimation of drug disposition properties by means of immobilized artificial membranes (IAM) and C18 columns, J. Med. Chem. 49 (2006) 4861–4870. https://doi.org/10.1021/jm0602108.

[13] M. Hidalgo-Rodríguez, S. Soriano-Meseguer, E. Fuguet, C. Ràfols, M. Rosés, Evaluation of the suitability of chromatographic systems to predict human skin permeation of neutral compounds, Eur. J. Pharm. Sci. 50 (2013) 557–568. https://doi.org/10.1016/j.ejps.2013.04.005.

[14] A.W. Sobańska, E. Brzezińska, IAM Chromatographic Models of Skin Permeation, Molecules. 27 (2022) 1893. https://doi.org/10.3390/molecules27061893.

[15] M. Janicka, Correlations between chromatographic parameters and bioactivity predictors of potential herbicides, J. Chromatogr. Sci. 52 (2014) 676–684. https://doi.org/10.1093/chromsci/bmt098.

[16] M. Janicka, M. Sztanke, K. Sztanke, Reversed-phase liquid chromatography with octadecylsilyl, immobilized artificial membrane and cholesterol columns in correlation studies with in silico biological descriptors of newly synthesized antiproliferative and analgesic active compounds, J. Chromatogr. A. 1318 (2013) 92–101. https://doi.org/10.1016/j.chroma.2013.09.060.

546 [17] M. Turowski, R. Kaliszan, Keratin immobilized on silica as a new stationary phase for
547 chromatographic modelling of skin permeation, J. Pharm. Biomed. Anal. 15 (1997) 1325–
548 1333. https://doi.org/10.1016/S0731-7085(96)02009-2.

549 [18] M. Turowski, R. Kaliszan, Collagen immobilised on silica derivatives as a new stationary
550 phase for HPLC, Biomed. Chromatogr. 12 (1998) 187–192.
551 https://doi.org/10.1002/(SICI)1099-0801(199807/08)12:4<187::AID-BMC727>3.0.CO;2-2.

552 [19] M.J. Ruiz-Ángel, S. Carda-Broch, J.R. Torres-Lapasió, M.C. García-Álvarez-Coque, Retention
553 mechanisms in micellar liquid chromatography, J. Chromatogr. A. 1216 (2009) 1798–1814.
554 https://doi.org/10.1016/j.chroma.2008.09.053.

555 [20] J.J. Martínez-Pla, Y. Martín-Biosca, S. Sagrado, R.M. Villanueva-Camañas, M.J. Medina-
556 Hernández, Biopartitioning micellar chromatography to predict skin permeability, Biomed.
557 Chromatogr. 17 (2003) 530–537. https://doi.org/10.1002/bmc.281.

558 [21] J.J. Martínez-Pla, Y. Martín-Biosca, S. Sagrado, R.M. Villanueva-Camañas, M.J. Medina-
559 Hernández, Evaluation of the pH effect of formulations on the skin permeability of drugs by
560 biopartitioning micellar chromatography, J. Chromatogr. A. 1047 (2004) 255–262.
561 https://doi.org/10.1016/j.chroma.2004.07.011.

562 [22] L.J. Waters, Y. Shahzad, J. Stephenson, Modelling skin permeability with micellar liquid
563 chromatography, Eur. J. Pharm. Sci. 50 (2013) 335–340.
564 https://doi.org/10.1016/j.ejps.2013.08.002.

565 [23] V. Dobričić, K. Nikolic, S. Vladimirov, O. Čudina, Biopartitioning micellar chromatography as
566 a predictive tool for skin and corneal permeability of newly synthesized 17β-carboxamide
567 steroids, Eur. J. Pharm. Sci. 56 (2014) 105–112. https://doi.org/10.1016/j.ejps.2014.02.007.

568 [24] A.W. Sobańska, J. Robertson, E. Brzezińska, Application of RP-18 TLC retention data to the
569 prediction of the transdermal absorption of drugs, Pharmaceuticals. 14 (2021) 147.
570 https://doi.org/10.3390/ph14020147.

[25] A.W. Sobańska, J. Robertson, E. Brzezińska, RP-18 TLC chromatographic and computational study of skin permeability of steroids, Pharmaceuticals. 14 (2021) 600. https://doi.org/10.3390/ph14070600.

[26] A.W. Sobańska, E. Brzezińska, RP-18 TLC and computational descriptors of skin permeability of sunscreens, Skin Pharmacol. Physiol. 35 (2022) 174–179. https://doi.org/10.1159/000522366.

[27] D.P. Poe, Theory of Supercritical Fluid Chromatography, in: C.F. Poole (Ed.), Supercritical Fluid Chromatography, Elsevier, Amsterdam, The Netherlands, 2017: pp. 23–55.

[28] L. Nováková, A. Grand-Guillaume Perrenoud, I. Francois, C. West, E. Lesellier, D. Guillarme, Modern analytical supercritical fluid chromatography using columns packed with sub-2μm particles: A tutorial, Anal. Chim. Acta. 824 (2014) 18–35. https://doi.org/10.1016/j.aca.2014.03.034.

[29] A. Tarafder, Metamorphosis of supercritical fluid chromatography to SFC: An Overview, Trends Anal. Chem. 81 (2016) 3–10. https://doi.org/10.1016/j.trac.2016.01.002.

[30] C. Galea, D. Mangelings, Y. Vander Heyden, Characterization and classification of stationary phases in HPLC and SFC - A review, Anal. Chim. Acta. 886 (2015) 1–15. https://doi.org/10.1016/j.aca.2015.04.009.

[31] C.F. Poole, Stationary phases for packed-column supercritical fluid chromatography, J. Chromatogr. A. 1250 (2012) 157–171. https://doi.org/10.1016/j.chroma.2011.12.040.

[32] C. West, E. Lemasson, S. Bertin, P. Hennig, E. Lesellier, An improved classification of stationary phases for ultra-high performance supercritical fluid chromatography, J. Chromatogr. A. 1440 (2016) 212–228. https://doi.org/10.1016/j.chroma.2016.02.052.

[33] C. Galea, D. Mangelings, Y. Vander Heyden, Method development for impurity profiling in SFC: The selection of a dissimilar set of stationary phases, J. Pharm. Biomed. Anal. 111 (2015) 333–343. https://doi.org/10.1016/j.jpba.2014.12.043.

[34] Y. Grooten, A. Sych, D. Mangelings, Y. Vander Heyden, Comparison of in-silico modelling and reversed-phase liquid chromatographic retention on an octadecyl silica column to predict skin permeability of pharmaceutical and cosmetic compounds, J. Pharm. Biomed. Anal. 201 (2021) 114095. https://doi.org/10.1016/j.jpba.2021.114095.

[35] Y. Grooten, Q. Marcelis, D. Mangelings, Y. Vander Heyden, Evaluating micellar liquid chromatographic methods on octadecyl particle-based and monolithic columns to predict the skin permeation of drug and cosmetic molecules, J. Chromatogr. A. 1663 (2022) 462753. https://doi.org/10.1016/j.chroma.2021.462753.

[36] Y. Grooten, D. Mangelings, Y. Vander Heyden, Predicting skin permeability of pharmaceutical and cosmetic compounds using retention on octadecyl, cholesterol-bonded and immobilized artificial membrane columns, J. Chromatogr. A. 1676 (2022) 463271. https://doi.org/10.1016/j.chroma.2022.463271.

[37] C. Muscat Galea, A. Slosse, D. Mangelings, Y. Vander Heyden, Investigation of the effect of column temperature and back-pressure in achiral supercritical fluid chromatography within the context of drug impurity profiling, J. Chromatogr. A. 1518 (2017) 78–88. https://doi.org/10.1016/j.chroma.2017.08.008.

[38] B.E. Vecchia, A.L. Bunge, Skin Absorption Databases and Predictive Equations, in: R.H. Guy, J. Hadgraft (Eds.), Transdermal Drug Delivery, Marcel Dekker, New York, USA, 2003: pp. 57–141.

[39] I.T. Degim, W.J. Pugh, J. Hadgraft, Skin permeability data: anomalous results, Int. J. Pharm. 170 (1998) 129–133. https://doi.org/10.1016/S0378-5173(98)00113-6.

[40] A.F. Azarbayjani, H. Lin, C.W. Yap, Y.W. Chan, S.Y. Chan, Surface tension and wettability in transdermal delivery: a study on the in-vitro permeation of haloperidol with cyclodextrin across human epidermis, J. Pharm. Pharmacol. 62 (2010) 770–778. https://doi.org/10.1211/jpp.62.06.0014.

[41] J. Thomas, S. Majumdar, S. Wasdo, A. Majumdar, K.B. Sloan, The effect of water solubility of solutes on their flux through human skin in vitro: an extended Flynn database fitted to the Roberts-Sloan equation, Int. J. Pharm. 339 (2007) 157–167. https://doi.org/10.1016/j.ijpharm.2007.02.031.

[42] K.T. Hoang, Dermal Exposure Assessment: Principles and Applications, Environmental Protection Agency, Office of Health and Environmental Assessment, EPA/600/8–91/011B, Washington, DC, USA, 1992.

[43] A. D'Attoma, C. Grivel, S. Heinisch, On-line comprehensive two-dimensional separations of charged compounds using reversed-phase high performance liquid chromatography and hydrophilic interaction chromatography. Part I: Orthogonality and practical peak capacity considerations, J. Chromatogr. A. 1262 (2012) 148–159. https://doi.org/10.1016/j.chroma.2012.09.028.

[44] A. Pedretti, L. Villa, G. Vistoli, VEGA - an open platform to develop chemo-bio-informatics applications, using plug-in architecture and script programming, J. Comput. Aided. Mol. Des. 18 (2004) 167–173. https://doi.org/10.1023/b:jcam.0000035186.90683.f2.

[45] S. Kim, J. Chen, T. Cheng, A. Gindulyte, J. He, S. He, Q. Li, B.A. Shoemaker, P.A. Thiessen, B. Yu, L. Zaslavsky, J. Zhang, E.E. Bolton, PubChem 2019 update: improved access to chemical data, Nucleic Acids Res. 47 (2019) D1102–D1109. https://doi.org/10.1093/nar/gky1033.

[46] VCCLAB (Virtual Computational Chemistry Laboratory), E-Dragon, (2005). http://www.vcclab.org (accessed December 2, 2019).

[47] J.P.M. Andries, G.H. Tinnevelt, Y. Vander Heyden, Improved modelling for low-correlated multiple responses by common-subset-of-independent-variables partial-least-squares, Talanta. 239 (2022) 123140. https://doi.org/10.1016/j.talanta.2021.123140.

[48] J.P.M. Andries, Y. Vander Heyden, L.M.C. Buydens, Improved variable reduction in partial least squares modelling based on Predictive-Property-Ranked Variables and adaptation of partial least squares complexity, Anal. Chim. Acta. 705 (2011) 292–305. https://doi.org/10.1016/j.aca.2011.06.037.

[49] D.L. Massart, B.G.M. Vandeginste, L.M.C. Buydens, S. De Jong, P.J. Lewi, J. Smeyers-Verbeke, Handbook of Chemometrics and Qualimetrics, Part A, Elsevier, Amsterdam, The Netherlands, 1997.

[50] Q. Gros, J. Molineau, A. Noireau, J. Duval, T. Bamba, E. Lesellier, C. West, Characterization of stationary phases in supercritical fluid chromatography including exploration of shape selectivity, J. Chromatogr. A. 1639 (2021) 461923. https://doi.org/10.1016/j.chroma.2021.461923.

[51] R.O. Potts, R.H. Guy, Predicting skin permeability, Pharm. Res. 9 (1992) 663–669. https://doi.org/10.1023/A:1015810312465.

[52] B.G.M. Vandeginste, D.L. Massart, L.M.C. Buydens, S. De Jong, P.J. Lewi, J. Smeyers-Verbeke, Handbook of Chemometrics and Qualimetrics: Part B, Elsevier, Amsterdam, The Netherlands, 1998.